Research Square

Preprints are preliminary reports that have not undergone peer review.
They should not be considered conclusive, used to inform clinical practice,
or referenced by the media as validated information.

Title：Cold-induced ethylene signaling activates the GmERF043-GmSACPD-C module to enhance cold tolerance in soybean

Han Gao
Jilin University
Xiangyang Chu
Jilin University
Yasong Feng
Jilin University
Xueyin Tang
Jilin University
Yajing Liu
Jilin University
Ying Wang
Jilin University
Jingwen Li
Jilin University
Hong Lu
Jilin Provincial Agricultural Technology Extension Station
Qingyu Wang
Jilin University
Fan Yan
fenfeiyongyuan@163.com
Jilin University

Research Article

Keywords: Soybean, Low-temperature stress, Ethylene, GmERF043, GmSACPD-C, Unsaturated fatty acids

Posted Date: November 12th, 2026

DOI: https://doi.org/10.21203/rs.3.rs-11453883/v1

License: This work is licensed under a Creative Commons Attribution 4.0 International License.
Read Full License

Additional Declarations: No competing interests reported.

Title： Cold-induced ethylene signaling activates the GmERF043-GmSACPD-C module to enhance cold tolerance in soybean

Han Gao[1#], Xiangyang Chu[1#], Yasong Feng[1], Xueyin Tang[1], Yajing Liu[1], Ying Wang[1], Jingwen Li[1], Hong Lu[2], Qingyu Wang[1]*, Fan Yan[1]*

Affiliations:

[1]College of Plant Science, Jilin University, Changchun 130062, China

[2] Jilin Provincial Agricultural Technology Extension Station, Changchun 130033, China

[#]**First authors:**

Han Gao: gaohan0718@163.com

Xiangyang Chu: 18037030571@163.com

They contributed equally to this work.

***Corresponding authors:**

Qingyu Wang: qywang@jlu.edu.cn

Fan Yan: fenfeiyongyuan@163.com

Abstract

Cold stress is a major abiotic stress restricting soybean (*Glycine max* L.) growth, development, and yield. Fatty acid metabolism is a core pathway in plant cold acclimation, and unsaturated fatty acids are essential substrates and regulators of cold tolerance; however, their upstream regulatory mechanisms remain poorly understood. *GmSACPD-C* encodes a seed-specific Δ9-stearoyl-ACP desaturase (SACPD，SAD) that converts stearic acid (C18:0) to oleic acid (C18:1) and primarily modulates seed fatty acid composition. Reduced *GmSACPD-C* activity decreases oleic acid levels. However, its role in soybean cold tolerance remains unclear. Through physiological measurements, yeast one-hybrid assays, genetic transformation, and integrated multi-omics analyses, this study demonstrates that cold-induced ethylene signaling, acting through the transcription factor *GmERF043* (ethylene responsive factor, ERF), upregulates *GmSACPD-C* expression to promote desaturation of saturated fatty acids, thereby preserving membrane fluidity and enhancing cold tolerance. *GmSACPD-C* promotes accumulation of unsaturated fatty acids and cold-responsive lipids, maintaining lipid homeostasis under low temperature. Mechanistic analyses revealed that GmERF043 directly binds the *GmSACPD-C* promoter and activates its transcription. *GmERF043* and *GmSACPD-C* show consistent effects on cold-tolerance phenotypes and lipid metabolism, and both are induced by ethylene signaling. We identified the GmERF043-GmSACPD-C regulatory module and propose that ethylene signaling participates in the soybean cold-stress response through transcriptional regulation of lipid metabolic pathways. These findings advance understanding of soybean cold-stress mechanisms, expand knowledge of ERF and SACPD stress-response functions, and provide genetic resources for molecular breeding of cold-tolerant soybean

Keywords: Soybean; Low-temperature stress; Ethylene; GmERF043; GmSACPD-C; Unsaturated

fatty acids

Introduction

Soybean (*Glycine max* L.) is an important global grain and oilseed crop and a major agricultural commodity (Liu et al., 2020), with considerable value as a source of food, industrial products, and forage (Duan et al., 2026; Vianna et al., 2023). It plays a strategically important role in ensuring global grain and oil security, improving human dietary patterns, and promoting agricultural development (Duan et al., 2025). The identification, characterization, and utilization of soybean germplasm with stable yield, high quality, and stress tolerance have long been key objectives in advancing soybean breeding (Shahzad et al., 2026; Shi et al., 2025). Soybean growth, development, and yield are often constrained by various abiotic stresses, including extreme temperatures, drought, and salinity. Among these stresses, chilling injury severely restricts the geographical range of soybean cultivation, impairs seedling growth, and causes substantial yield losses; therefore, it is considered a major adverse environmental factor limiting stable cultivation and sustainable soybean production (Liu et al., 2024; Tsegaw et al., 2023).

Chilling stress, a globally prevalent abiotic stress, generally restricts the suitable cultivation zones and ecological adaptability of various crops and severely affects plant morphogenesis, physiological metabolism, yield, and quality. This stress represents a major adverse factor constraining stable yield increases and crop quality improvement worldwide (Li et al., 2025; Sun et al., 2018). Low-temperature stress disrupts cellular redox homeostasis, inhibits antioxidant enzyme activity, and triggers excessive accumulation of reactive oxygen species (ROS), leading to oxidative cellular damage and programmed cell death (X. Zhang et al., 2025). It also disrupts osmoprotectant metabolism, fatty acid homeostasis, and photosynthetic carbon metabolism; inhibits photosynthesis and energy production; and impedes cell division and plant morphogenesis. Collectively, these alterations ultimately lead to retarded plant growth, leaf wilting, and developmental arrest (Goswami et al., 2022), thereby severely compromising crop yield and quality. Accordingly, elucidating the molecular mechanisms underlying plant cold responses and identifying key functional genes associated with cold tolerance are critical for understanding plant stress adaptation mechanisms, developing new cold-tolerant crop cultivars, and ensuring stable food production under climate change scenarios.

Ethylene is a key endogenous phytohormone that plays a central role in regulating plant growth and development, metabolism, and abiotic stress responses (Aragón-Raygoza & Strable, 2025; Dubois et al., 2018; Huang et al., 2024; Li et al., 2024; Zhong et al., 2014). As an essential signaling molecule, ethylene plays a crucial role in plant responses to low-temperature stress (Huang et al., 2023). Ethylene enhances plant antioxidant capacity and maintains cellular membrane integrity by modulating the transcription of a set of downstream functional genes, thereby positively regulating plant cold tolerance (Sabir et al., 2026). The ethylene response factor PtrERF9 perceives ethylene signals and modulates ROS homeostasis via PtrGSTU17, thereby promoting cold tolerance in *Poncirus trifoliata* (L.) (Zhang et al., 2022). In cotton, GhDREB1 enhances the expression of the ethylene biosynthetic gene GhACO1, thereby promoting cold tolerance (Dong et al., 2025). In rice, ethylene negatively regulates cold tolerance through CONSTITUTIVE TRIPLE RESPONSE1 (CTR1) and CTR2 by repressing abscisic acid (ABA)-induced stomatal closure (Huang et al., 2025). The VvbHLH30-VvERF70-VvACS2 module positively regulates cold tolerance in grape by promoting ethylene accumulation (Hou et al., 2026). In apple, the MdGLK1–MdBZR1 module integrates ethylene and strigolactone signals to regulate cold tolerance through a CBF-dependent pathway (X. W. Zhang et al., 2025). Overall, ethylene and its associated signaling pathways play crucial roles in regulating plant cold tolerance. Nevertheless, few studies have focused on the ethylene-mediated regulation of cold tolerance in soybean, and the underlying molecular mechanisms

remain largely unknown.

The biological membrane serves as the primary barrier protecting plant cells against environmental stresses and plays essential roles in physiological processes, including molecular and ion transport, signal perception, and the maintenance of intracellular homeostasis (Shomo et al., 2024). The relative abundance of saturated and unsaturated fatty acids in membrane lipids is a pivotal physicochemical determinant of the membrane phase-transition temperature and plant cold adaptability (Zhang et al., 2019). Saturated fatty acids possess relatively straight carbon chains and strong intermolecular interactions that facilitate close molecular packing under low-temperature conditions, thereby promoting phase transitions in cell membranes. These phase transitions lead to increased membrane rigidity and permeability and intracellular solute leakage, consequently impairing plant cold tolerance. In contrast, unsaturated fatty acids introduce bends into carbon chains, hinder the ordered packing of membrane lipid molecules, effectively lower the critical temperature for membrane lipid phase transitions, and maintain membrane fluidity and structural integrity under cold stress (Zhang et al., 2024; Zhou et al., 2025).

Currently, research on plant cold acclimation has largely focused on the CBF/DREB-dependent pathway, whereas the hormone-mediated dynamic regulation of membrane lipids remains underexplored. Although ethylene accumulation under cold stress has been documented, its downstream transcriptional regulatory network and direct targets involved in lipid metabolism remain unclear, limiting a comprehensive understanding of the chilling response in soybean. To address this knowledge gap, the present study focuses on key transcription factors downstream of ethylene signaling and aims to systematically elucidate the mechanisms underlying enhanced cold tolerance through the complete cascade of "signal perception–transcriptional activation-lipid remodeling." This work is expected not only to address the specific knowledge gap regarding ethylene-mediated regulation of membrane lipid unsaturation but also to provide new insights into how crops actively remodel cellular physical barriers to cope with cold stress, thereby offering important fundamental insights into plant cold adaptation.

In this study, the full-length coding sequence (CDS) of *GmSACPD-C* was cloned based on the latest soybean reference genome (Glycine max Wm82.a6.v1). Bioinformatics analyses were performed for homologous sequence alignment and phylogenetic analysis. Haplotype analysis revealed that *GmSACPD-C* was subject to artificial selection during soybean domestication and that its natural allelic variation was significantly associated with unsaturated fatty acid content. We systematically characterized the biological role of *GmSACPD-C* in soybean cold tolerance using stable *GmSACPD-C*-overexpressing (OE) transgenic lines and *GmSACPD-C* RNA interference (RNAi) in soybean hairy roots. Multiple physiological indices associated with cold stress, including phenotypic changes, cell membrane damage, osmoprotectant content, and antioxidant enzyme activities, were analyzed; moreover, elite cold-tolerant soybean materials were developed.

Furthermore, we demonstrated that the ethylene response factor GmERF043 directly activates *GmSACPD-C* transcription to enhance cold tolerance in soybean. We propose a hierarchical ethylene-GmERF043-GmSACPD-C regulatory module that clarifies the molecular mechanism by which ethylene signaling modulates soybean cold tolerance through the GmERF043-GmSACPD-C cascade. Our results refine the regulatory network underlying ethylene-mediated cold-stress responses in soybean, elucidate the coordinated roles of ethylene signaling and fatty acid metabolism in regulating cold tolerance, and provide a solid theoretical basis for developing elite soybean germplasm with high oleic acid content and cold tolerance.

Results

GmSACPD-C encodes a highly conserved desaturase preferentially expressed in seeds

To characterize the fundamental molecular features of *GmSACPDs* associated with the regulation of cold-stress responses in soybean, five *GmSACPDs* were analyzed, with seven *AtSADs* from *Arabidopsis thaliana* used as references. Phylogenetic analysis revealed high sequence homology between *GmSACPDs* and *AtSADs*. *GmSACPD-C* exhibited the highest homology to the functionally important *Arabidopsis* gene *AtFTM1* (also designated *AtAAD6*, *AtSAD6*, *AtHUP7*, and *AT3G02610*) (Figure 1A). This gene encodes a chloroplast-localized stearoyl-ACP Δ9 desaturase that catalyzes the conversion of stearoyl-ACP to oleoyl-ACP and serves as a key regulatory component of unsaturated fatty acid biosynthesis. Conserved-domain prediction indicated that, similar to AtSADs, GmSACPD-C harbors the characteristic domain of plant stearoyl-ACP Δ9 desaturases (PLN00179), which represents the core region responsible for the fatty acid desaturase activity of the SAD family (Figure 1B). This finding suggests that plant stearoyl-acyl-carrier-protein desaturases (SAD/SACPDs) have a highly conserved catalytic role in unsaturated fatty acid production.

GmSACPD-C shows a tissue-specific expression profile. Its transcript abundance was substantially higher in developing seeds than in vegetative organs (roots, stems, and leaves) and flowers. *GmSACPD-C* expression increased substantially with seed development, peaking at the R6 seed-filling stage and declining slightly at the R7 beginning-maturity stage. Nevertheless, its transcript level remained significantly higher at R7 than at the early seed-filling stage (R5) and in all tested vegetative and reproductive tissues (Figure 1C). This expression pattern suggests a critical role for *GmSACPD-C* during soybean seed development. Subcellular localization assays confirmed that GmSACPD-C localizes in chloroplasts (Figure 1D), the primary sites of de novo fatty acid synthesis in plants. This localization is consistent with the subcellular localization of its *Arabidopsis* homolog AtFTM1 and with the biochemical function of GmSACPD-C in catalyzing stearoyl-ACP desaturation.

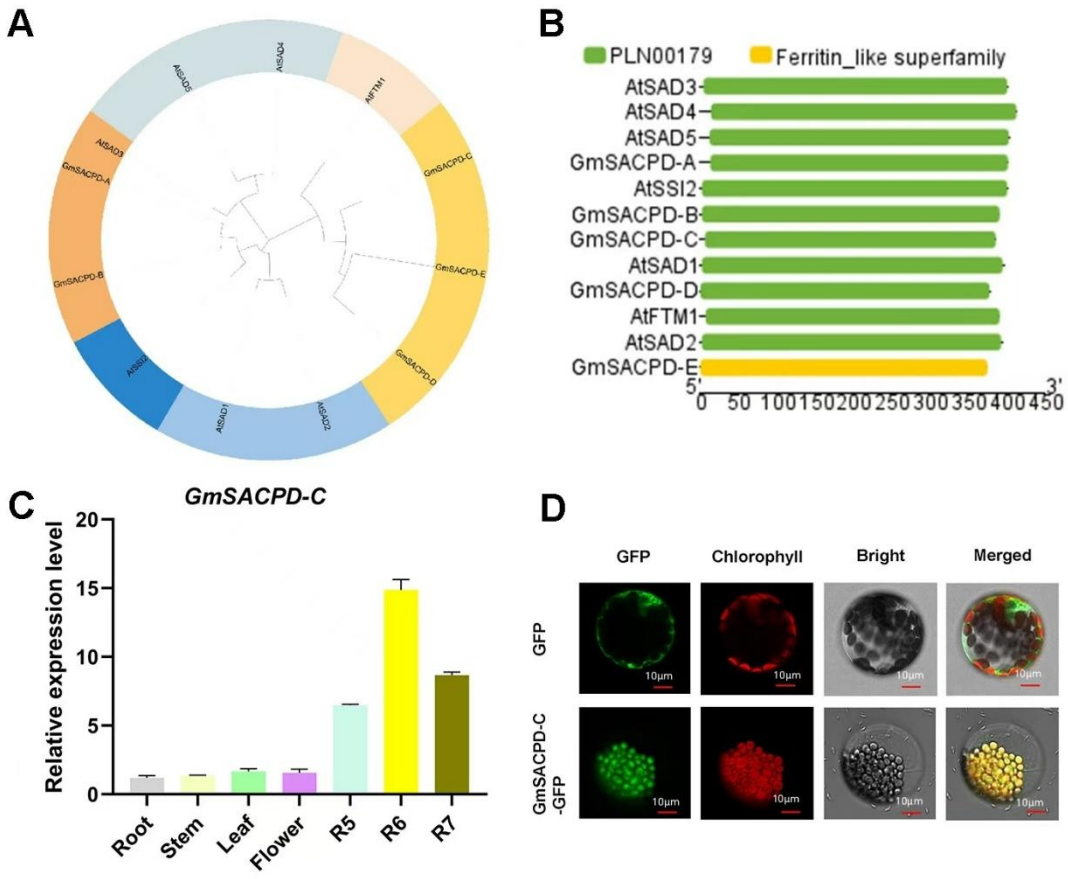


Figure 1. GmSACPD-C encodes a highly conserved desaturase that is predominantly expressed in seeds. (A) Phylogenetic tree of SACPD proteins from different species. (B) Schematic representation of the conserved domain architecture of SACPDs. (C) Spatiotemporal expression profiling of *GmSACPD-C* in various tissues and developmental stages. The data include three biological replicates, each with three technical replicates. (D) Subcellular localization of the GmSACPD-C in protoplast of Arabidopsis. Bar = 10 μm.

Haplotype analysis of *GmSACPD-C*

To investigate the selection pattern of *GmSACPD-C* during domestication, genetic analysis of *GmSACPD-C* was performed using the SoyOmics big-data platform. Four *GmSACPD-C* haplotypes were identified across a domestication-gradient panel encompassing wild soybeans, landraces, and improved cultivars. The four haplotypes occurred at relatively similar frequencies among wild soybean accessions. Among landraces, HAP2 was enriched during domestication, whereas the frequencies of HAP3 and HAP4 gradually declined. Only two predominant haplotypes, HAP1 and HAP2, were retained in modern improved cultivars, whereas HAP3 and HAP4 were nearly lost during breeding selection (Figure 2A). Phenotype-association analysis revealed that HAP3 was associated with low unsaturated fatty acid content, which was significantly lower than that of HAP1 and HAP2 (Figure 2B). The four *GmSACPD-C* haplotypes were differentiated by combinations of three key single-nucleotide polymorphisms (SNPs): two located in noncoding regions (T to G and A to C) and one within the coding region (T to C) (Figure 2C). The SNP in the coding region causes a nonsynonymous substitution of aspartic acid with glutamic acid, which may have contributed to the rapid positive selection of HAP2 during the transition from wild soybeans to landraces. Negative Tajima's D values were detected across the full-length gene region in all three populations. Wild soybeans exhibited higher genetic diversity than landraces and improved cultivars, suggesting that *GmSACPD-C* has undergone persistent purifying selection during soybean domestication. The population differentiation index F_{ST} indicated substantially greater genetic differentiation between wild soybeans and improved cultivars than between landraces and improved cultivars, suggesting that directional artificial selection during breeding contributed to shifts in haplotype frequencies at this locus (Figure 2D).

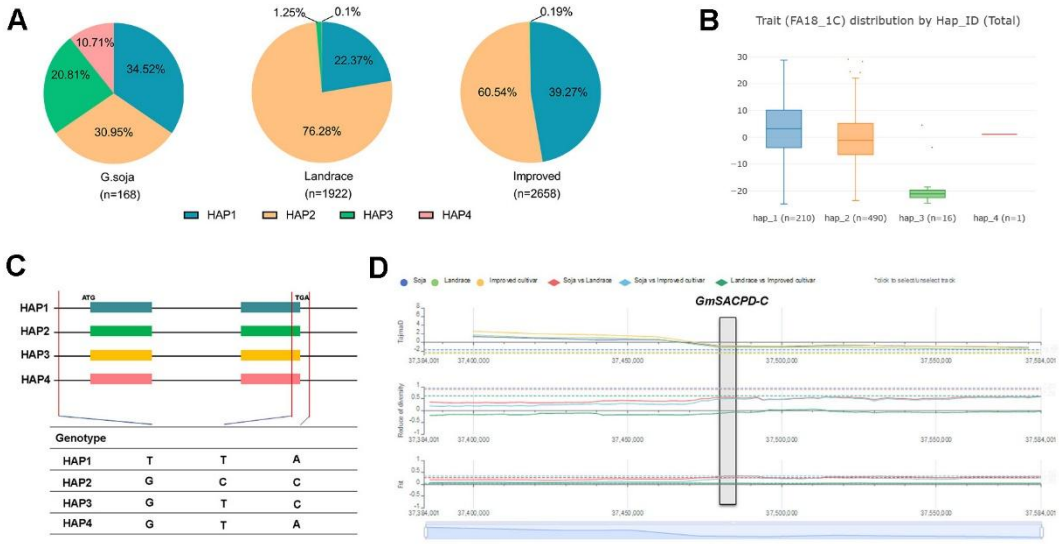


Figure 2. Haplotype analysis. (A) Frequency distribution of haplotypes among different soybean populations. (B) Distribution of the trait (FA18_1C) across different haplotypes. (C) Schematic

representation of haplotype structures and genotypic variations. (D) Genome-wide association analysis of the genomic region.

GmSACPD-C promotes the biosynthesis of unsaturated fatty acids

To validate the genetic function of *GmSACPD-C*, the CaMV35S::*GmSACPD-C* construct was generated and introduced into the soybean cultivar Dongnong50 (DN50) via *Agrobacterium tumefaciens*-mediated cotyledonary-node transformation. Two overexpression lines (*GmSACPD-C*-OE1 and *GmSACPD-C*-OE2) exhibited stable inheritance (Figure 3A) and were propagated in the field to the T_3 generation for subsequent phenotypic assays. Seeds of the *GmSACPD-C*-OE lines were markedly larger and had greater seed width than their wild-type (WT) counterparts (Figures 3B and 3C). Statistical analysis confirmed that 100-seed weight was significantly higher in both OE lines and positively correlated with *GmSACPD-C* transcript levels (Figure 3D). These results suggest that *GmSACPD-C* overexpression modulates seed-related agronomic traits in soybean.

Subsequently, gas chromatography was used to quantify the fatty acid profiles of mature seeds. The contents of palmitic acid (C16:0), stearic acid (C18:0), oleic acid (C18:1), linoleic acid (C18:2), and linolenic acid (C18:3) were all significantly higher in *GmSACPD-C*-OE seeds than in their WT counterparts (Figures 3E-3I). Furthermore, *GmSACPD-C*-RNAi hairy roots were generated in the DN50 background via *Agrobacterium rhizogenes*-mediated transformation (Figure S1) for fatty acid quantification. In contrast to the overexpression lines, the contents of palmitic acid (C16:0), stearic acid (C18:0), oleic acid (C18:1), linoleic acid (C18:2), and linolenic acid (C18:3) were significantly lower in *GmSACPD-C*-RNAi hairy roots (Figures 3J-3N). Overall, GmSACPD-C, a key enzyme involved in unsaturated fatty acid biosynthesis, promotes oleic acid biosynthesis and modulates fatty acid metabolism in soybean.

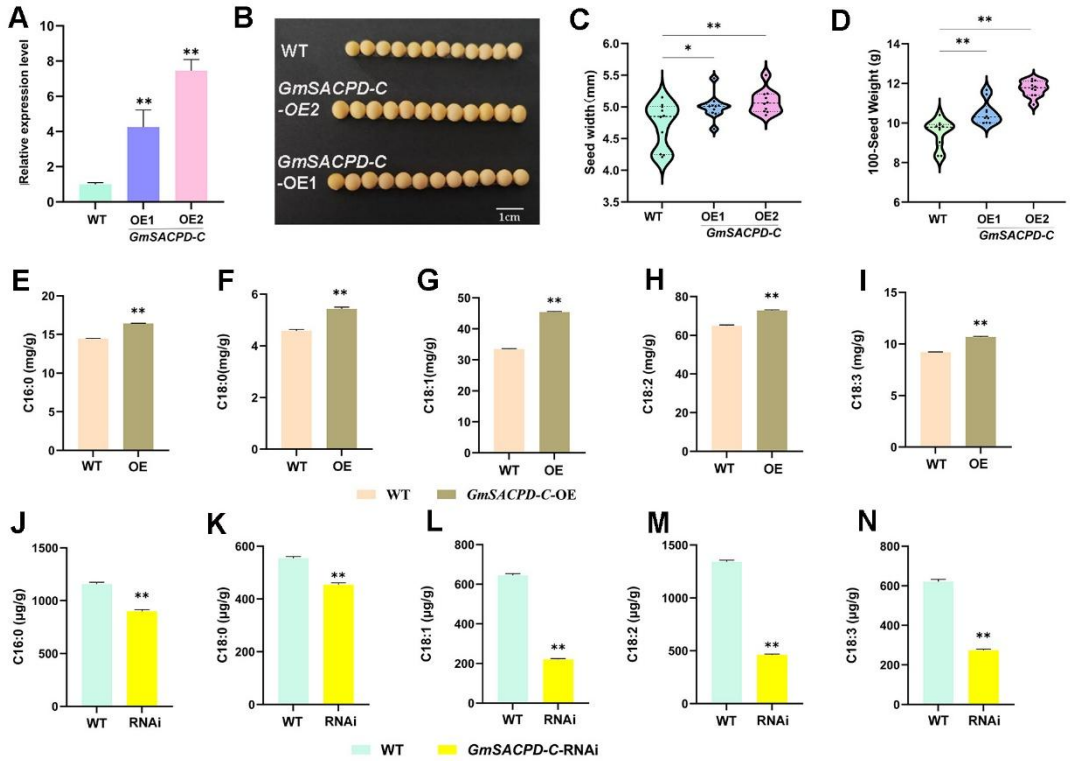


Figure 3. GmSACPD-C promotes unsaturated fatty acid biosynthesis. (A) Identification of WT and overexpression lines. The data include three biological replicates, each with three technical replicates. (B) Morphology of seeds from WT and overexpression lines. Bar = 1cm. (C-D) Seed

width (C), 100-seed weight (D) of WT and overexpression lines. (E) C16:0 content in seeds of WT and overexpression lines. (F) C18:0 content in seeds of WT and overexpression lines. (G) C18:1 content in seeds of WT and overexpression lines. (H) C18:2 content in seeds of WT and overexpression lines. (I) C18:3 content in seeds of WT and overexpression lines. (J) C16:0 content in seeds of WT and overexpression lines. (K) C18:0 content in WT and RNAi hairy roots. (L) C18:1 content in WT and RNAi hairy roots. (M) C18:2 content in WT and RNAi hairy roots. (N) C18:3 content in WT and RNAi hairy roots. Data were analyzed by one-way ANOVA, * represents $P < 0.05$, ** represents $P < 0.01$.

GmSACPD-C enhances cold tolerance in soybean

GmSACPD catalyzes the conversion of saturated fatty acids to unsaturated fatty acids. Unsaturated fatty acid content is a critical determinant of plant cold tolerance. To characterize the cold-stress-responsive expression pattern of *GmSACPD-C*, wild-type (WT) soybean seedlings were subjected to cold treatment at 4 °C. Quantitative real-time PCR (qPCR) was performed to analyze *GmSACPD-C* expression in soybean leaves and roots at 0, 3, 6, 12, 24, and 48 h after exposure to low temperature. Cold stress significantly upregulated *GmSACPD-C* expression in both leaves and roots, with transcript levels initially increasing and subsequently decreasing under prolonged stress. In leaves, *GmSACPD-C* expression peaked during the early stage of cold treatment and gradually declined thereafter but remained significantly higher than the control level at 12 h (Figure 4A). In roots, *GmSACPD-C* expression peaked at 3 h and subsequently decreased but remained significantly higher than the control level at 12 h (Figure 4B). These data demonstrate that *GmSACPD-C* expression is responsive to cold stress in soybean.

To systematically investigate the biological function of GmSACPD-C in the cold-stress response, WT soybean plants, *GmSACPD-C*-OE transgenic lines, and composite *GmSACPD-C*-RNAi plants were used as experimental materials and subjected to low-temperature treatment at 4 °C. Morphological changes in leaves and roots were recorded after the cold treatment. Physiological indices, including electrolyte leakage; root length; root-to-shoot ratio; catalase (CAT), superoxide dismutase (SOD), and peroxidase (POD) activities; and malondialdehyde (MDA), proline (PRO), and hydrogen peroxide (H_2O_2) contents, were measured. With prolonged cold treatment, the leaves of WT plants gradually wilted, developed chlorosis and necrotic lesions, and curled. In contrast, cold-induced injury symptoms appeared later and were less severe in the *GmSACPD-C*-OE lines (Figure 4C). Primary root length and fresh- and dry-weight root-to-shoot ratios did not differ significantly between the overexpression lines and WT plants under cold conditions (Figures S2A and S2D-S2F). Moreover, root growth-related parameters remained unchanged in *GmSACPD-C*-RNAi composite plants (Figures S2B and S2G-S2I). These observations suggest that *GmSACPD-C* may not participate in the cold-stress response by modulating root elongation or root-to-shoot biomass partitioning.

Physiological assays revealed that SOD and POD activities were markedly higher in *GmSACPD-C*-OE lines than in WT plants at 24 and 48 h under cold stress (Figures 4E and 4F). At 48 h after cold exposure, *GmSACPD-C*-OE lines accumulated significantly lower levels of MDA but higher levels of Pro than their WT counterparts (Figures 4G and 4H). In contrast, *GmSACPD-C*-RNAi composite plants exhibited cold-induced damage earlier, and the damage was more severe than that in controls (Figure S2C). Consistently, MDA content was significantly higher in *GmSACPD-C*-RNAi plants at 24 and 48 h of cold stress (Figure 4N). Moreover, POD activity was substantially higher in *GmSACPD-C*-OE lines and significantly lower in *GmSACPD-C*-RNAi plants under cold treatment, suggesting that *GmSACPD-C* contributes to limiting excessive ROS accumulation (Figures 4I and 4P). Membrane integrity analysis demonstrated that root electrolyte leakage was significantly lower in *GmSACPD-C*-OE lines but higher

in *GmSACPD-C*-RNAi plants than in WT plants (Figures 4J and 4Q). Because electrolyte leakage reflects the extent of membrane damage, these results indicate that elevated *GmSACPD-C* expression alleviates cold-induced root membrane injury, whereas *GmSACPD-C* silencing aggravates cold-induced membrane damage and electrolyte leakage. Therefore, *GmSACPD-C* contributes to maintaining membrane integrity under low-temperature conditions.

Lipidomic profiling revealed significantly greater accumulation of multiple cold-responsive lipid species in the roots of cold-stressed *GmSACPD-C*-OE plants than in WT controls. Phosphatidic acid (PA) species PA (16:0_18:1) and PA (33:2) were significantly enriched in the overexpression lines (Figures S3A and S3B), indicating that *GmSACPD-C* overexpression promotes PA accumulation. For phosphatidylcholine (PC), the relative abundance of polyunsaturated PC (32:4) increased significantly in OE plants, whereas that of ether-linked PC (O-31:0) decreased to a very low level, suggesting species-specific remodeling within the PC pool (Figures S3C and S3D). Two phosphatidylethanolamine (PE) species, PE (40:3) and PE (33:2), were significantly more abundant in *GmSACPD-C*-OE roots (Figures S3E and S3F). Furthermore, several phosphatidylglycerol (PG) species, including PG (16:3_16:0), PG (O-17:3_18:4), PG (P-15:2_16:2), and PG (O-18:2_21:2), exhibited significant or highly significant increases in the overexpression lines (Figures S3G-S3J). Collectively, these findings demonstrate that *GmSACPD-C* overexpression facilitates the accumulation of PA and PE species and regulates the remodeling of PG lipids, thereby reshaping the membrane lipid profile. Thus, our results support the conclusion that *GmSACPD-C* positively modulates soybean cold tolerance by promoting the accumulation of cold-adaptive unsaturated lipids and inducing membrane lipid remodeling.

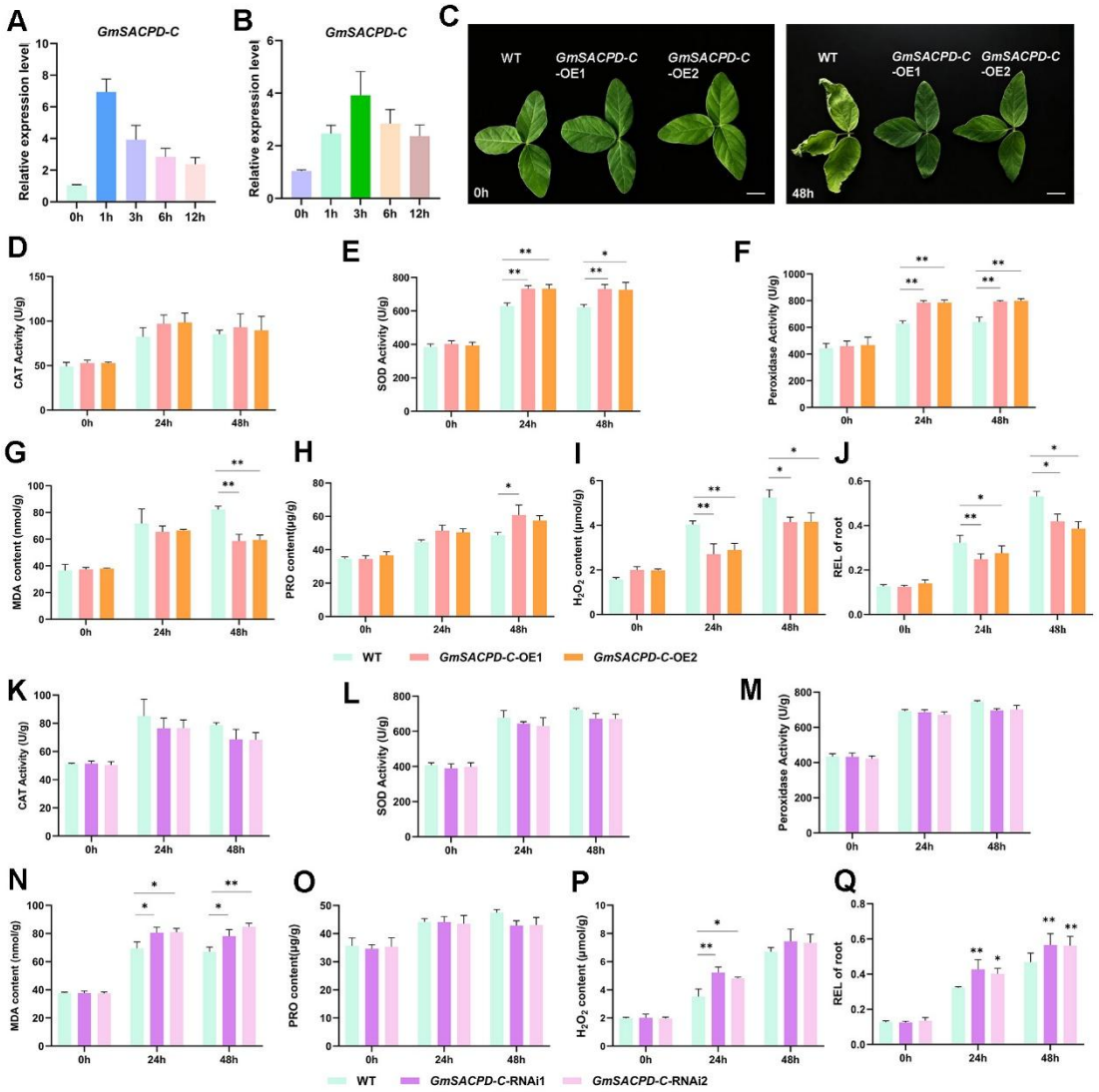


Figure 4. GmSACPD-C positively regulates cold tolerance in soybean. (A) Relative expression levels of *GmSACPD-C* in leaves under low-temperature stress at different treatment times. (B) Relative expression levels of *GmSACPD-C* in roots under low-temperature stress at different treatment times. (C) Leaf morphology under low-temperature stress at different treatment times. Bar =1cm. (D) CAT activity in roots of *GmSACPD-C*-OE and WT under low-temperature stress at different treatment times. (E) SOD activity in roots of *GmSACPD-C*-OE and WT. (F) POD activity in roots of *GmSACPD-C*-OE and WT. (G) MDA content in roots of *GmSACPD-C*-OE and WT. (H) PRO content in roots of *GmSACPD-C*-OE and WT. (I) H_2O_2 content in roots of *GmSACPD-C*-OE and WT. (J) REL in roots of *GmSACPD-C*-OE and WT. (K) CAT activity in roots of *GmSACPD-C*-RNAi and WT. (L) SOD activity in roots of *GmSACPD-C*-RNAi and WT. (M) POD activity in roots of *GmSACPD-C*-RNAi and WT. (N) MDA content in roots of *GmSACPD-C*-RNAi and WT. (O) PRO content in roots of *GmSACPD-C*-RNAi and WT. (P) H_2O_2 content in roots of *GmSACPD-C*-RNAi and WT. (Q) REL in roots of *GmSACPD-C*-RNAi and WT. The data include three biological replicates, each with three technical replicates. Data were analyzed by one-way ANOVA, * represents $P < 0.05$, ** represents $P < 0.01$.

GmERF043 directly activates *GmSACPD-C* expression to enhance cold tolerance in soybean

Although previous studies have demonstrated close links between plant SACPDs and cold tolerance, the underlying regulatory mechanisms remain poorly understood. To elucidate the molecular mechanism underlying *GmSACPD-C*-mediated regulation of cold tolerance in soybean, cis-element prediction was performed on the GmSACPD-C promoter. An ethylene-responsive element, a putative binding site for ethylene response factors, was identified (Figure S4A). An ethylene response factor, designated GmERF043 according to the Wm82.a6.v1 genome annotation, was identified as a candidate regulator of the *GmSACPD-C* promoter. Conserved-domain analysis revealed that *GmERF043* harbors a characteristic AP2 DNA-binding domain (Figure S4B). For yeast one-hybrid assays, the full-length CDS of *GmERF043* was cloned into the pB42AD vector to generate the prey construct, whereas the *GmSACPD-C* promoter fragment was inserted into pLacZi to generate the bait construct. Yeast one-hybrid assays confirmed that GmERF043 binds to the *GmSACPD-C* promoter in yeast (Figures 5A and 5B). Next, the full-length CDS of GmERF043 was inserted into pCHF3300 to generate a CaMV35S::*GmERF043* effector plasmid. Meanwhile, the *GmSACPD-C* promoter fragment was cloned into pGreen II 0800 to generate the reporter construct *pGmSACPD-C*-LUC (Figure 5C). The reporter plasmid was co-infiltrated with either the effector plasmid or the empty-vector control into *Nicotiana benthamiana* leaves for transient expression. The dual-luciferase assay revealed that *GmERF043* significantly enhanced the transcriptional activity of the *GmSACPD-C* promoter (Figures 5D and 5E).

ERF proteins are key transcription factors in the ethylene signaling pathway and participate broadly in diverse stress responses. To investigate the response of GmERF043 to cold stress, WT (DN50) seedlings were treated at 4 °C. QPCR was used to quantify *GmERF043* transcript abundance in leaves and roots at 0, 1, 3, 6, and 12 h after cold exposure. Cold stress substantially upregulated *GmERF043* expression in both leaves and roots, with transcript levels initially increasing and subsequently declining. In leaves, *GmERF043* expression peaked at 3 h and gradually decreased but remained significantly higher than the control level at 12 h (Figure 5F). In roots, transcript levels peaked at 1 h and subsequently declined but remained significantly higher than the control level at 12 h (Figure 5G), confirming that *GmERF043* expression is responsive to cold stress in soybean.

To characterize the biological function of *GmERF043*, overexpression and RNAi-silencing constructs were generated and introduced via Agrobacterium rhizogenes-mediated transformation to obtain *GmERF043*-OE and *GmERF043*-RNAi composite soybean plants (Figures 5H and 5I). QPCR revealed that *GmSACPD-C* transcript levels were significantly higher in *GmERF043*-OE plants and significantly lower in *GmERF043*-RNAi plants than in their respective controls (Figures 5J and 5K). This expression pattern suggests that GmERF043 serves as an important upstream regulator of *GmSACPD-C* under cold stress. WT, *GmERF043*-OE, and *GmERF043*-RNAi composite soybean plants were subjected to cold treatment at 4 °C. After prolonged cold exposure, the leaves of control plants exhibited progressive wilting, chlorosis, curling, and necrosis. Injury symptoms appeared later and were less severe in *GmERF043*-OE plants, whereas *GmERF043*-RNAi plants exhibited the opposite phenotype (Figure S4C). Primary root length and fresh- and dry-weight root-to-shoot ratios did not differ significantly among genotypes under cold conditions (Figures S4D-S4G). Similar to *GmSACPD-C*, *GmERF043* may not contribute to the cold-stress response by regulating root elongation or root-to-shoot biomass partitioning. CAT activity was significantly higher in *GmERF043*-OE plants at 24 and 48 h of low-temperature treatment, whereas it was significantly lower in *GmERF043*-RNAi plants at 24 h (Figure 5L). SOD activity was higher in *GmERF043*-OE plants at 24 h and lower in *GmERF043*-RNAi plants at 48 h (Figure 5M). *GmERF043*-OE plants exhibited higher POD activity at both 24 and 48 h,

whereas POD activity was significantly lower in *GmERF043*-RNAi plants (Figure 5N). Under cold stress, MDA content was significantly lower in *GmERF043*-OE plants at 24 and 48 h (Figure 5O), whereas Pro content was significantly higher in *GmERF043*-OE plants at 48 h (Figure 5P). Furthermore, H_2O_2 content and root electrolyte leakage were measured. At 24 and 48 h of cold treatment, H_2O_2 content was significantly lower in *GmERF043*-OE plants and higher in *GmERF043*-RNAi plants (Figure 5Q). Root electrolyte leakage was significantly lower in *GmERF043*-OE plants but higher in *GmERF043*-RNAi plants than in their WT counterparts (Figure 5R). Collectively, these results indicate that GmERF043 directly activates *GmSACPD-C* transcription. Under cold-stress conditions, GmERF043 enhances cold tolerance in soybean by upregulating *GmSACPD-C* expression, reduced the electrolyte leakage rate under cold stress, enhancing ROS-scavenging capacity, and alleviating oxidative damage.

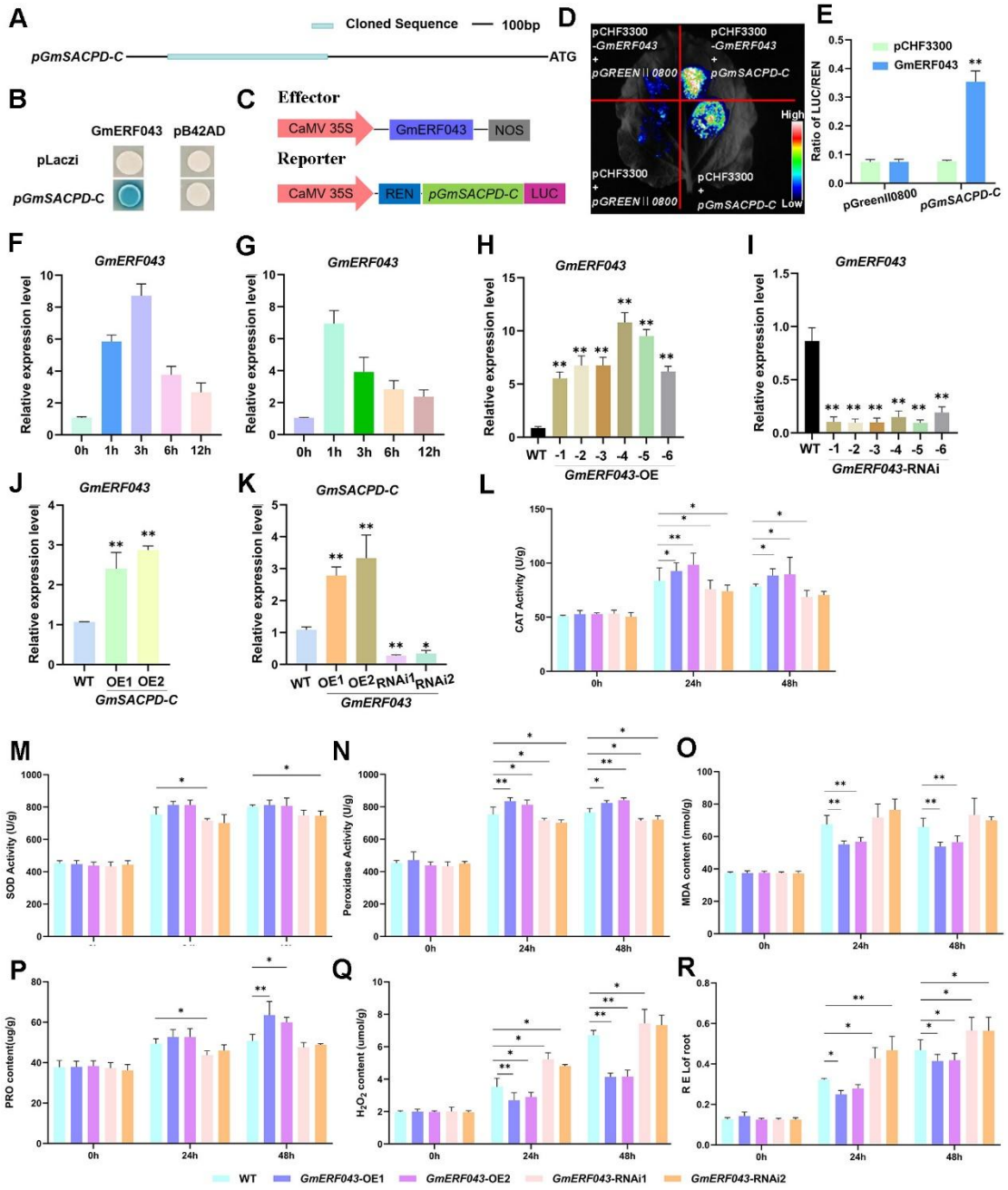


Figure 5. GmERF043 directly promotes *GmSACPD-C* expression to enhance cold tolerance in

soybean. (A) Schematic diagram of the *GmSACPD-C* promoter. (B) Yeast one-hybrid assay verified that GmERF043 directly binds to the promoter of *GmSACPD-C*. (C) Schematic representation of the vector construction. (D-E) Luciferase reporter assay for *GmSACPD-C* and *GmERF043*. (F) Relative expression levels of *GmERF043* in leaves under low-temperature stress at different treatment times. (G) Relative expression levels of *GmERF043* in roots under low-temperature stress at different treatment times. (H) Identification of *GmERF043*-overexpressing hairy roots. (I) Identification of *GmERF043*-RNAi hairy roots. (J) Expression of *GmERF043* in *GmSACPD-C* -OE lines. (K) Expression of *GmSACPD-C* in *GmERF043* transgenic lines. (L) CAT activity in hairy roots of *GmERF043*-OE/RNAi and WT under low-temperature stress at different treatment times. (M) SOD activity in hairy roots of *GmERF043*-OE/RNAi and WT. (N) POD activity in hairy roots of *GmERF043*-OE/RNAi and WT. (O) MDA content in hairy roots of *GmERF043*-OE/RNAi and WT. (P) PRO content in hairy roots of *GmERF043*-OE/RNAi and WT. (Q) H_2O_2 content in hairy roots of *GmERF043*-OE/RNAi and WT. (R) REL in hairy roots of *GmERF043*-OE/RNAi and WT. The data include three biological replicates, each with three technical replicates. Data were analyzed by one-way ANOVA, * represents $P < 0.05$, ** represents $P < 0.01$.

The *GmERF043-GmSACPD-C* module potentially mediates ethylene-dependent regulation of cold tolerance in soybean

Ethylene is a multifunctional stress-related hormone that plays important roles in plant cold-stress responses; however, its function varies among species. Members of the ERF family serve as key transcription factors involved in ethylene signaling. Given that *GmERF043* is cold-responsive, we hypothesized that the ethylene signaling pathway participates in the cold-stress response in soybean. To test this hypothesis, we examined the transcript levels of key ethylene biosynthesis genes under cold-stress conditions. Cold stress significantly induced the expression of *GmACS*1 and *GmACO2*, which play crucial roles in ethylene biosynthesis, with their expression peaking at 1 h after cold treatment. Subsequently, *GmACS1* expression steadily decreased, with only a slight rebound at 6 h. In contrast, *GmACO2* expression decreased after 1 h, increased again from 6 h to 12 h, and declined markedly at 24 h (Figures 6A and 6B). These observations indicate that key genes involved in ethylene biosynthesis are coordinately activated during the early stage of cold stress.

Subsequently, WT soybean seedlings were treated with 0.2 mM 1-aminocyclopropane-1-carboxylic acid (ACC), the biosynthetic precursor of ethylene, and the temporal expression profiles of *GmERF043* and *GmSACPD-C* were analyzed. *GmERF043* and *GmSACPD-C* displayed highly similar responses to exogenous ACC. The transcript levels of both genes gradually increased relative to their respective levels at 0 h, peaked at 3 h, subsequently declined, showed a slight increase at 12 h, and decreased significantly at 24 h (Figures 6C and 6D). These results demonstrate that exogenous ACC induces both *GmERF043* and *GmSACPD-C* expression, suggesting that the two genes are coordinately regulated in response to ethylene signaling.

Overall, cold stress rapidly upregulates *GmACS1* and *GmACO2* expression, suggesting activation of ethylene biosynthesis. Exogenous ACC treatment further supports the involvement of ethylene signaling in the coordinated expression of the transcription factor-encoding gene *GmERF043* and the fatty acid desaturase gene *GmSACPD-C*. Therefore, we propose a working model in which cold stress induces ethylene biosynthesis in soybean. Increased ethylene signaling induces *GmERF043* expression, and *GmERF043* subsequently activates *GmSACPD-C* transcription. GmSACPD-C, a stearoyl-ACP desaturase, promotes unsaturated fatty acid biosynthesis, increases the proportion of unsaturated fatty

acids in membrane lipids, lowers the membrane phase-transition temperature, and alleviates cold-induced membrane damage, thereby enhancing cold tolerance in soybean (Figure 6E). In summary, the *GmERF043-GmSACPD-C* module represents a potential regulatory node mediating ethylene-dependent cold tolerance in soybean.

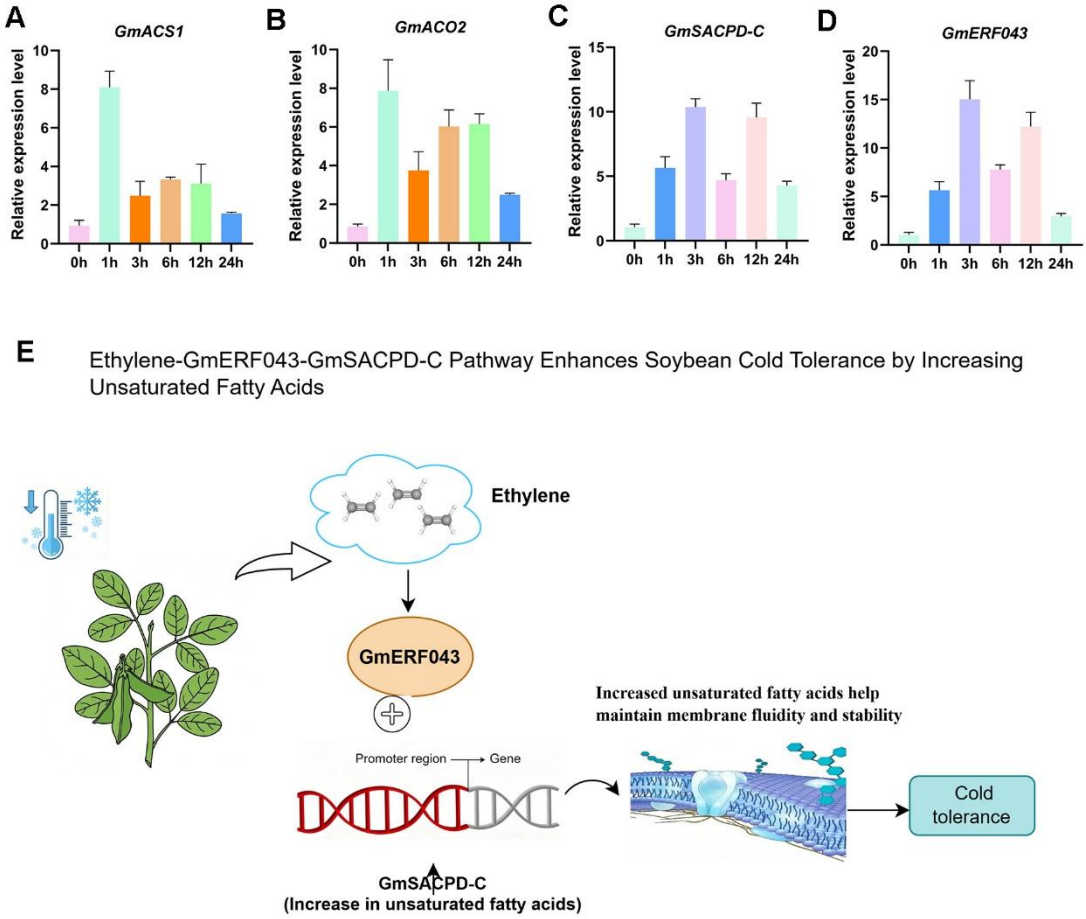


Figure 6. The *GmERF043-GmSACPD-C* module is a potential mediator of ethylene signaling in regulating soybean cold tolerance. (A) Relative expression levels of *GmACS1* under low-temperature stress at different treatment times. (B) Relative expression levels of *GmACO2* under low-temperature stress at different treatment times. (C) Relative expression levels of *GmSACPD-C* at different treatment times following ACC application. (D) Relative expression levels of *GmERF043* at different treatment times following ACC application. The data of (A-D) include three biological replicates, each with three technical replicates. (E) A schematic model illustrating that the *GmERF043-GmSACPD-C* module mediates ethylene signaling to regulate cold tolerance in soybean.

Discussion

Chilling injury refers to physiological damage caused by low-temperature conditions above 0 °C in thermophilic plants. A primary event underlying chilling injury is the transition of membrane lipids from a liquid-crystalline state to a gel state, resulting in increased membrane permeability and electrolyte leakage (Barrero-Sicilia et al., 2017; Dhaliwal & Angeles-Shim, 2022). This transition triggers a cascade of adverse consequences, including inhibition of photosynthesis and respiration,

physiological drought caused by impaired root water uptake, oxidative damage resulting from ROS bursts, disruption of osmotic adjustment, and altered protein metabolism. These changes lead to growth retardation, leaf chlorosis, wilting, and yield loss (Qian et al., 2024). As a thermophilic crop, soybean is susceptible to chilling stress at the seedling stage, which represents a major abiotic constraint on seedling emergence, photosynthetic efficiency, and final yield (Hussain et al., 2022; Tsegaw et al., 2023).

The ICE-CBF (DREB1) -COR cascade represents a well-characterized pathway associated with cold acclimation in soybean. Previous studies have demonstrated that *GmDREB1* responds to cold stress and activates the transcription of downstream genes by recognizing DRE cis-elements (Kidokoro et al., 2015). Ethylene signaling represses the CBF/DREB1 pathway at the transcriptional level via EIN3 (Robison et al., 2019). In addition, *GmSCOF-1* is induced by both ABA and low temperature and modulates COR gene expression by binding to ABRE motifs (Kim et al., 2001). Moreover, *GmICE1* directly activates *GmSPS8/18*, extending the canonical ICE1–CBF–COR cold-signaling cascade to sucrose biosynthesis and osmotic regulation (Shen et al., 2023). These findings demonstrate that the CBF-dependent regulatory network in soybean does not function in isolation but is intricately integrated with multiple intersecting signaling pathways. Several other physiological pathways also contribute to the regulation of cold tolerance. *GmSNAT1* enhances cold adaptation through melatonin biosynthesis, signal transduction, and downstream physiological protection (Ren et al., 2026). *GmbZIP44*, *GmbZIP62*, and *GmbZIP78* function as negative regulators of ABA signaling and promote chilling tolerance (Liao et al., 2008). Heterologous overexpression of *GmMYBJ1* in *A. thaliana* enhances cold tolerance (Su et al., 2014). MiRNAs, including *miR319*, *miR394*, *miR397*, and *miR398*, respond to cold stress and mediate post-transcriptional regulation (Hussain et al., 2022). Ectopic expression of *GmNAC20* also enhances cold tolerance in *Arabidopsis* (Hao et al., 2011).

The degree of fatty acid unsaturation in membrane lipids is a crucial determinant of chilling tolerance in plants. Plants adapt to low-temperature environments by remodeling membrane structure and physiological status through modulation of fatty acid composition, lipid metabolic pathways, and stress-responsive transcription factor networks. Under cold-stress conditions, GmFAD3A maintains appropriate linolenic acid levels through differential regulation of specific isoforms in the endoplasmic reticulum and plastids, thereby facilitating environmental adaptation (Román et al., 2012). Overexpression of *GmFAD3A* in rice alleviates oxidative damage by promoting proline accumulation and enhancing antioxidant enzyme activity, thereby enhancing cold tolerance and seed germination under cold-stress conditions (Wang et al., 2019). *GmSACPD-C* catalyzes the conversion of stearic acid to oleic acid and serves as a key enzyme involved in unsaturated fatty acid biosynthesis in soybean. Our results revealed that *GmSACPD-C* transcript levels were positively associated with unsaturated fatty acid content and cold-tolerance capacity. *GmSACPD-C* overexpression markedly increased the accumulation of unsaturated fatty acids and cold-responsive lipids and enhanced cold tolerance, whereas RNAi-mediated silencing produced the opposite phenotypes. These results identify *GmSACPD-C* as an important gene linking lipid metabolism to cold adaptation in soybean. *GmSACPD-C* positively modulates the cold-stress response by reshaping lipid profiles and promoting the accumulation of stress-associated lipid species. These findings are consistent with reports from classical model systems showing that unsaturated fatty acid biosynthesis contributes to chilling tolerance and provide new insights into the functions of the SACPD family under abiotic stress.

Furthermore, we elucidated the upstream regulatory cascade of *GmSACPD-C* and demonstrated that the ERF transcription factor GmERF043 directly binds to the *GmSACPD-C* promoter and activates its transcription. ERF proteins serve as important transcriptional regulators of stress responses and are broadly involved in hormone signaling and adaptation to abiotic stress. The consistent cold-stress phenotypes of *GmERF043* and *GmSACPD-C* transgenic lines provide genetic evidence supporting the role of GmERF043 in enhancing cold tolerance through activation of *GmSACPD-C* transcription. Identification of this regulatory module reveals a mechanism underlying the transcriptional activation of *GmSACPD-C* and provides insight into its upstream regulation. In addition to their well-documented roles in stress signal transduction, our findings indicate that ERF transcription factors can participate in cold-stress responses by modulating lipid metabolic pathways, thereby broadening our understanding of the biological functions of *ERFs*.

Ethylene is a major stress-responsive phytohormone that plays an important role in cold tolerance and growth homeostasis. Nevertheless, the molecular mechanism by which ethylene signaling coordinates lipid metabolism to modulate cold-stress responses remains unclear. Our data support ethylene-responsive transcriptional induction of both *GmERF043* and *GmSACPD-C*. Based on their regulatory relationship, we propose an ethylene-dependent cold-tolerance cascade in which ethylene signaling induces *GmERF043* expression, which in turn activates *GmSACPD-C* transcription and promotes the biosynthesis and accumulation of unsaturated fatty acids and cold-responsive lipids, thereby enhancing cold tolerance in soybean. This study identifies a potential ethylene-GmERF043-GmSACPD-C regulatory module involved in the cold-stress response, linking ethylene signaling with lipid metabolism and providing mechanistic insights into the regulation of cold tolerance in soybean. These conclusions are primarily based on phenotypic and molecular data obtained from seedlings under controlled conditions; the functional relevance of this module at other developmental stages and under field conditions requires further investigation. Moreover, direct binding of GmERF043 to the *GmSACPD-C* promoter, currently supported by yeast one-hybrid assays, requires in planta validation using chromatin immunoprecipitation.

Conclusion

In this study, we used soybean to elucidate the molecular regulatory mechanisms underlying cold tolerance, characterized the biological function of *GmSACPD-C* in enhancing cold tolerance in soybean, and elucidated its upstream transcriptional regulation. GmSACPD-C positively regulates cold tolerance in soybean by modulating the biosynthesis and metabolism of unsaturated fatty acids and cold-responsive lipids, thereby maintaining the structural and functional integrity of cell membranes under low-temperature conditions. The ethylene response factor GmERF043 directly binds to the *GmSACPD-C* promoter and activates its transcription; both genes contribute to the cold-stress response in soybean and are responsive to ethylene signaling. We identified a potential GmERF043-GmSACPD-C regulatory module involved in ethylene-dependent regulation of cold tolerance in soybean. These findings advance our understanding of the molecular regulatory network underlying the low-temperature stress response in soybean, expand knowledge of the stress-response functions of ERF transcription factors and SACPD family genes, provide new insights into the molecular basis of low-temperature adaptation in crops, and offer valuable candidate genes and a theoretical foundation for developing cold-tolerant germplasm and improving stress-tolerance traits through molecular breeding in soybean. Future work should further investigate the upstream signaling events linking ethylene perception to *GmERF* activation, potential crosstalk with other hormone signaling pathways, and the applicability of this regulatory

module under field conditions and in other legume crops.

Materials and Methods

Plant materials and growth conditions

Soybean (*Glycine max* L.) cultivars Williams.82 (W82) and Dongnong 50 (DN50) were used in this study. Transgenic *GmSACPD-C*-OE lines together with wild-type controls were planted in parallel. Two seeds were sown per hole, with 12.5 cm plant spacing and 65 cm row spacing to guarantee uniformity and reproducibility of field trials. Tobacco (*Nicotiana benthamiana*) was cultivated in an artificial climate chamber under 24 °C with a 16 h light , 8 h dark photoperiod; light intensity was set to 8000 lx (white-light LED).

Gene cloning and bioinformatic analysis

Total RNA was isolated from immature embryos of Williams.82, and cDNA was synthesized by reverse transcription using the PrimeScript RT kit. The full-length coding sequence of *GmSACPD-C* (*Glyma.14G141200*) was amplified using the synthesized cDNA as template. The PCR program was set as follows: initial denaturation at 94 °C for 5 mins, 28 cycles of 94 °C for 30 s, 60 °C for 30 s, and 72 °C for 1 min, followed by a final extension for 10 mins. The amplified fragment (1161 bp) was ligated into the pMD18-T vector and subjected to Sanger sequencing. Sequence alignment confirmed complete consistency with the reference sequence in public databases.

Information concerning the ORF length, exon-intron organization and deduced amino-acid length of *GmSACPD-C* was retrieved from the Phytozome database (https://phytozome-next.jgi.doe.gov/). Conserved protein domains were predicted via NCBI-CDD (Home - Conserved Domains - NCBI). Cis-acting elements within the 2000 bp upstream of the 5′-UTR of the GmSACPD-C promoter were analyzed using PlantCARE (PlantCARE, a database of plant promoters and their cis-acting regulatory elements). Multiple-sequence alignment and phylogenetic analysis (Neighbor-Joining method) were performed with TBtools and MEGA 11.0.

Subcellular localization of *GmSACPD-C*

The vector pCAMBIA3301-GmSACPDC-2×flag-GFP was constructed using seamless cloning. Rosette leaves were harvested from 3-4-week-old *Arabidopsis thaliana* (Col-0), and protoplasts were isolated via enzymatic digestion with Cellulase R-10 and Macerozyme R-10. The protoplasts were transiently transformed by the PEG-mediated method. After incubation at 25 °C in darkness for 20 h, GFP fluorescence signals were detected using a confocal laser scanning microscope.

Construction of expression vectors

The full-length CDS of *GmSACPD-C* and *GmERF043* were individually inserted into the *XbaI*/*SacI* restriction sites of the pTF101-35S vector to generate overexpression constructs pTF101-*GmSACPD-C* and pTF101-*GmERF043*. Meanwhile, specific fragments of *GmERF043* and *GmSACPD-C* were cloned into the pTF101-35S-pKannibal backbone to generate RNA interference (RNAi) constructs pTF101(RNAi)-*GmERF043* and pTF101(RNAi)-*GmSACPD-C*, respectively. All recombinant plasmids were verified by Sanger sequencing and stored at -20 °C for subsequent use.

Agrobacterium-mediated soybean cotyledon-node transformation

Soybean cultivar DN50 was used as the receptor material for Agrobacterium-tumefaciens-mediated genetic transformation. Explant preparation and selection procedures were performed according to Xu et al. (2022). Cotyledon explants were co-cultivated

for 3-4 d, then transferred onto shoot-induction medium containing 8 mg/L Basta for two-week selection, followed by subculture on selection medium with the same Basta concentration. Fresh medium was renewed every 14 d, and necrotic tissues were discarded. Resistant shoots were transferred to rooting medium to regenerate T_0 transformants. Primary screening was carried out by leaf painting with 160 mg/L glufosinate-ammonium, wild-type leaves exhibited chlorosis 7 d after treatment whereas transgenic lines remained normal. Positive transgenic plants were further validated by PCR amplification of the Bar gene and strip test.

Quantitative analysis of fatty-acid composition

Immature embryos at the R6 stage were harvested from T_2-generation *GmSACPD-C*-OE lines and wild-type controls for total lipid extraction. Fatty-acid methyl esters (FAMEs) were prepared via KOH-methanol transesterification. For samples difficult to esterify, acetyl chloride-methanol reflux method was adopted. FAMEs were analysed by GC-FID equipped with a 100 m high-polarity capillary column. The carrier-gas flow rate was set at 1.0 mL/min with a split ratio of 30:1, and a temperature-programmed elution was applied. A mixture of 37 fatty-acid methyl-ester standards was used for qualitative identification, and triundecanoin served as the internal standard for quantification. Fatty-acid profiles were determined in mature seeds of *GmSACPD-C*-OE, wild-type DN50 seeds, and RNAi hairy roots. One-way analysis of variance (ANOVA) was performed using SPSS software, and inter-group differences were assessed by LSD multiple-range test.

Lipidomic profiling

Each sample (0.5 g) was ground in liquid nitrogen, and total lipids were extracted using a modified Bligh-Dyer method. Lipid separation and detection were performed on a UHPLC-MS/MS system equipped with an ACQUITY UPLC CSH C18 column (2.1 mm × 100 mm, 1.7 μm). Data were acquired under both positive- and negative-ion modes. Raw data were converted via ProteoWizard, and lipid identification and quantification were carried out using LipidSearch software with internal-standard-based semi-quantification. After data normalization, principal-component analysis (PCA) and orthogonal partial least-squares-discriminant analysis (OPLS-DA) were conducted in MetaboAnalyst. Differential lipid metabolites were screened with thresholds of $VIP > 1$ and $P < 0.05$. Lipid metabolic-pathway enrichment and relative-abundance analysis were performed using the LIPID MAPS database.

Yeast one-hybrid assay

Vectors pLacZi2μ and pJG4-5 were digested by double restriction-enzyme digestion. The reaction was incubated at 37 °C for 3 h and terminated by adding 6 μL of 10 × loading buffer. Digested products were separated by 1 % agarose-gel electrophoresis, and target fragments were gel-purified. The full-length coding sequence of *GmERF043* was inserted into pJG4-5 by seamless cloning, while the promoter fragment of *GmSACPD-C* was cloned into pLacZi2μ. Recombinant plasmids were transformed into yeast competent cells (EGY48), and transformants were selected on SD/-Trp/-Ura plates. Randomly picked colonies were transferred onto chromogenic medium containing X-gal and incubated in the dark at 30 °C for 2-3 d to observe blue colony formation.

Dual-luciferase reporter assay

The full-length CDS of GmERF043 was cloned into pCAMBIA3300 to generate the effector construct pCAMBIA3300-*GmERF043*. The *GmSACPD-C* promoter fragment validated by yeast one-hybrid was inserted into pGreen II 0800 to produce the reporter construct pGreenII 0800-*pGmSACPD-C*. Each plasmid was transformed into Agrobacterium tumefaciens GV3101 and cultured until OD_{600} reached 0.6. Effector and reporter bacterial suspensions were

mixed at a 1:1 ratio and infiltrated into leaves of 4-week-old Nicotiana benthamiana. At 48 h after infiltration, 50 mg/L D-luciferin potassium salt was smeared onto the abaxial leaf surface. After 5 min incubation in the dark, chemiluminescence images were captured. The empty vector pGreenII 0800-LUC was used as the negative control. LUC and REN activities were quantitatively measured using a dual-luciferase assay kit (TransGen), and the LUC/REN ratio was used to evaluate the transcriptional-activation capacity of GmERF043. Each assay included no fewer than three biological replicates.

Cold-stress treatment and measurement of plant growth parameters

Soybean seeds were surface-sterilized and sown in sterilized vermiculite at a depth of 1.5 cm, and grown in an artificial climate chamber under a 16 h light, 8 h dark photoperiod. Seven days after emergence, seedlings were transferred to a hydroponic system for acclimation. When plants reached the three-leaf stage (V3), uniformly-grown seedlings were subjected to cold treatment at 4 °C. Tissue samples were harvested at 0, 1, 6, 12 and 24 h after cold exposure, with three biological replicates for each time-point. Upon completion of cold treatment, fresh weights of shoots and roots were recorded. Plant tissues were placed in labelled paper bags and oven-dried to constant weight (approximately two weeks) for dry-weight measurement. Root length, fresh weight and dry weight were recorded, and the root-to-shoot ratio was calculated as: root-to-shoot ratio = root dry weight / shoot dry weight. Three independent replicates were set for each treatment. Harvested samples were immediately frozen in liquid nitrogen and stored at -80 °C.

Exogenous ethylene treatment

Soybean seeds were sterilized and sown in nutrient soil, and cultivated in a greenhouse at 24 °C under a 16 h light, 8 h dark cycle. At the VC stage (when the first true leaf was fully expanded), seedlings were uniformly sprayed with 0.2 mM ACC solution (Sigma-Aldrich) until leaf surfaces were thoroughly wetted. The third trifoliate leaves were collected at 0, 1, 3, 6, 12 and 24 h post-treatment, snap-frozen in liquid nitrogen and stored at -80 °C for subsequent analyses. Each treatment contained three biological replicates, and each replicate consisted of three individual plants with consistent growth status.

Quantitative real-time PCR (qRT-PCR)

Gene expression analyses were performed using the SYBR Premix Ex Taq kit on a real-time PCR instrument. *GmActin11* was used as the reference gene. Relative expression levels were calculated by the $2^{-}\Delta\Delta Ct$ method. Each sample was assayed with three biological replicates and three technical replicates.

Hairy-root induction and transformation

Agrobacterium rhizogenes K599 harbouring target constructs (*GmERF043*-OE, *GmERF043*-RNAi and *GmSACPD-C*-RNAi) was activated by shaking culture at 28 °C in LB medium supplemented with spectinomycin and streptomycin. Cells at logarithmic growth phase were harvested and resuspended in infiltration solution (pH 5.7) containing 180 μM acetosyringone, adjusted to $OD_{600} = 0.8$, and incubated at room temperature for 2 h. Four-day-old germinated soybean seedlings were selected; oblique cuts were made on hypocotyls, which were immersed in bacterial suspension for 30 min, and extra bacterial suspension was injected into wound sites. After 5 d of co-cultivation, seedlings were transferred to hydroponic systems, and nutrient solution was renewed every 5 d. Transgenic hairy roots were harvested after two-week cultivation for subsequent assays. Genomic DNA was isolated from hairy roots, and transgene integration was verified by PCR amplification. RT-qPCR was further performed to detect transcript levels of target genes for

evaluating overexpression or silencing efficiency.

Measurement of electrolyte leakage

Fresh leaf tissues (0.1 g) were placed into 50 mL centrifuge tubes with 20 mL ultrapure water. Tissues were fully submerged by vacuum infiltration for 10 mins. Tissues were then transferred into 20 mL fresh ultrapure water and incubated for 1 h, after which the initial electrical conductivity was measured using a conductivity meter. Samples were subsequently boiled for 10 min and cooled to room temperature to record the final electrical conductivity. Relative electrolyte leakage (%) = (initial conductivity / final conductivity) × 100 %.

Determination of antioxidant and osmotic-adjustment parameters

Activities of superoxide dismutase (SOD), peroxidase (POD) and catalase (CAT) were determined using Solarbio assay kits (BC0170, BC0090, BC0205). Contents of hydrogen peroxide (H_2O_2), proline and malondialdehyde (MDA) were measured with Solarbio kits BC3595, BC0295 and BC6410, respectively. All operations were strictly performed according to the manufacturer's instructions. Three biological replicates were included for each physiological parameter.

Funding

The work was supported in part by the National Natural Science Foundation of China (32472180), Natural Science Foundation of Jilin Province (20240101260JC).

Declarations

Conflict of interest: The authors declare no conflict of interest.

Accession numbers

Sequence data for the genes analyzed in this study can be found in SoyBase (https://www.soybase.org) and Phytozome (https://phytozome-next.jgi.doe.gov) under the following locus identifiers: *GmSACPD-C*(Glyma.14G121400), *GmERF043* (Glyma.17G254600), *GmACS1*(Glyma.07G128000), *GmACO2*(Glyma.08G029200).

References

Aragón-Raygoza, A., & Strable, J. (2025). Diverse roles of ethylene in maize growth and development, and its importance in shaping plant architecture. *J Exp Bot*, *76*(7), 1854-1865. https://doi.org/10.1093/jxb/eraf062

Barrero-Sicilia, C., Silvestre, S., Haslam, R. P., & Michaelson, L. V. (2017). Lipid remodelling: Unravelling the response to cold stress in Arabidopsis and its extremophile relative Eutrema salsugineum. *Plant Sci*, *263*, 194-200. https://doi.org/10.1016/j.plantsci.2017.07.017

Dhaliwal, L. K., & Angeles-Shim, R. B. (2022). Cell Membrane Features as Potential Breeding Targets to Improve Cold Germination Ability of Seeds. *Plants (Basel)*, *11*(23). https://doi.org/10.3390/plants11233400

Dong, Y., Ma, H., Shen, Y., Li, P., Ge, C., Shen, Q., Li, J., Liu, R., Zhang, S., Liu, S., & Pang, C. (2025). Ethylene enhances cold resistance through GhDREB1/CBF in cotton (Gossypium hirsutum L.). *Plant J*, *124*(1), e70517. https://doi.org/10.1111/tpj.70517

Duan, Z., Fang, C., Liu, S., Nian, H., Zhou, G., & Tian, Z. (2026). Soybean. *Curr Biol*, *36*(9), R370-r374. https://doi.org/10.1016/j.cub.2026.03.039

Duan, Z., Xu, L., Zhou, G., Zhu, Z., Wang, X., Shen, Y., Ma, X., Tian, Z., & Fang, C. (2025). Unlocking soybean potential: genetic resources and omics for breeding. *J Genet Genomics*, *52*(11), 1337-1346. https://doi.org/10.1016/j.jgg.2025.02.004

Dubois, M., Van den Broeck, L., & Inzé, D. (2018). The Pivotal Role of Ethylene in Plant Growth. *Trends Plant Sci*, *23*(4), 311-323. https://doi.org/10.1016/j.tplants.2018.01.003

Goswami, A. K., Maurya, N. K., Goswami, S., Bardhan, K., Singh, S. K., Prakash, J., Pradhan, S., Kumar, A., Chinnusamy, V., Kumar, P., Sharma, R. M., Sharma, S., Bisht, D. S., & Kumar, C. (2022). Physio-biochemical and molecular stress regulators and their crosstalk for low-temperature stress responses in fruit crops: A review. *Front Plant Sci*, *13*, 1022167. https://doi.org/10.3389/fpls.2022.1022167

Hao, Y. J., Wei, W., Song, Q. X., Chen, H. W., Zhang, Y. Q., Wang, F., Zou, H. F., Lei, G., Tian, A. G., Zhang, W. K., Ma, B., Zhang, J. S., & Chen, S. Y. (2011). Soybean NAC transcription factors promote abiotic stress tolerance and lateral root formation in transgenic plants. *Plant J*, *68*(2), 302-313. https://doi.org/10.1111/j.1365-313X.2011.04687.x

Hou, Y., Wong, D. C. J., Wang, L., Kang, Y., Zhou, H., Kafle, S., Liu, Y., Xu, M., Meng, L., Liang, Z., Yu, G., Wang, Q., & Xin, H. (2026). A Hierarchical VvbHLH30-VvERF70-VvACS2 Module Orchestrates Ethylene Biosynthesis and Cold Adaptation in Grapevine. *Plant Biotechnol J*, *24*(6), 4317-4341. https://doi.org/10.1111/pbi.70640

Huang, J., Zhao, X., Bürger, M., Chory, J., & Wang, X. (2023). The role of ethylene in plant temperature stress response. *Trends Plant Sci*, *28*(7), 808-824. https://doi.org/10.1016/j.tplants.2023.03.001

Huang, S., Wang, H., Liu, S., Lu, S., Hua, J., & Zou, B. (2025). Ethylene antagonizes ABA and inhibits stomatal closure and chilling tolerance in rice. *J Exp Bot*, *76*(17), 5011-5024. https://doi.org/10.1093/jxb/eraf052

Huang, W., Tan, C., & Guo, H. (2024). Ethylene in fruits: beyond ripening control. *Hortic Res*, *11*(10), uhae229. https://doi.org/10.1093/hr/uhae229

Hussain, M. A., Li, S., Gao, H., Feng, C., Sun, P., Sui, X., Jing, Y., Xu, K., Zhou, Y., Zhang, W., & Li, H. (2022). Comparative analysis of physiological variations and genetic architecture for cold stress response in soybean germplasm. *Front Plant Sci*, *13*, 1095335. https://doi.org/10.3389/fpls.2022.1095335

Kidokoro, S., Watanabe, K., Ohori, T., Moriwaki, T., Maruyama, K., Mizoi, J., Myint Phyu Sin Htwe, N., Fujita, Y., Sekita, S., Shinozaki, K., & Yamaguchi-Shinozaki, K. (2015). Soybean DREB1/CBF-type transcription factors function in heat and drought as well as cold stress-responsive gene expression. *Plant J*, *81*(3), 505-518. https://doi.org/10.1111/tpj.12746

Kim, J. C., Lee, S. H., Cheong, Y. H., Yoo, C. M., Lee, S. I., Chun, H. J., Yun, D. J., Hong, J. C., Lee, S. Y., Lim, C. O., & Cho, M. J. (2001). A novel cold-inducible zinc finger protein from soybean, SCOF-1, enhances cold tolerance in transgenic plants. *Plant J*, *25*(3), 247-259. https://doi.org/10.1046/j.1365-313x.2001.00947.x

Li, H., Wang, S., Zhai, L., Cui, Y., Tang, G., Huo, J., Li, X., & Bian, S. (2024). The miR156/SPL12 module orchestrates fruit colour change through directly regulating ethylene production pathway in blueberry. *Plant Biotechnol J*, *22*(2), 386-400. https://doi.org/10.1111/pbi.14193

Li, R., Zheng, C. F., Liu, B., Hu, C., Song, Y., Fu, H., Zhang, H., Zhang, C., Zhu, Q. H., & Jiang, M. (2025). OsbZIP83-OsCOMT15 module confers melatonin-ameliorated cold tolerance in rice. *Plant J*, *123*(3), e70402. https://doi.org/10.1111/tpj.70402

Liao, Y., Zou, H. F., Wei, W., Hao, Y. J., Tian, A. G., Huang, J., Liu, Y. F., Zhang, J. S., & Chen, S. Y. (2008). Soybean GmbZIP44, GmbZIP62 and GmbZIP78 genes function as negative regulator of ABA signaling and confer salt and freezing tolerance in transgenic Arabidopsis. *Planta*, *228*(2), 225-240. https://doi.org/10.1007/s00425-008-0731-3

Liu, S., Zhang, M., Feng, F., & Tian, Z. (2020). Toward a "Green Revolution" for Soybean. *Mol Plant*, *13*(5), 688-697. https://doi.org/10.1016/j.molp.2020.03.002

Liu, X., Zhang, C., Lamlom, S. F., Zhao, K., Abdelghany, A. M., Wang, X., Zhang, F., Yuan, R., Han, D., Zha, B., Lu, W., Ren, H., & Zhang, B. (2024). Genetic Adaptations of Soybean to Cold Stress Reveal Key Insights Through Transcriptomic Analysis. *Biology (Basel)*, *13*(11). https://doi.org/10.3390/biology13110856

Qian, Z., He, L., & Li, F. (2024). Understanding cold stress response mechanisms in plants: an overview. *Front Plant Sci*, *15*, 1443317. https://doi.org/10.3389/fpls.2024.1443317

Ren, C., Cheng, T., Zhang, W., Chen, S., Zhang, S., Zhao, Q., Cao, L., Zhang, Y., & Yu, G. (2026). GmSNAT1 enhances cold tolerance in soybean by promoting melatonin biosynthesis and interacting with GmPSYR1. *Plant Physiol*. https://doi.org/10.1093/plphys/kiag516

Robison, J. D., Yamasaki, Y., & Randall, S. K. (2019). The Ethylene Signaling Pathway Negatively Impacts CBF/DREB-Regulated Cold Response in Soybean (Glycine max). *Front Plant Sci*, *10*, 121. https://doi.org/10.3389/fpls.2019.00121

Román, Á., Andreu, V., Hernández, M. L., Lagunas, B., Picorel, R., Martínez-Rivas, J. M., & Alfonso, M. (2012). Contribution of the different omega-3 fatty acid desaturase genes to the cold response in soybean. *J Exp Bot*, *63*(13), 4973-4982. https://doi.org/10.1093/jxb/ers174

Sabir, I. A., Hu, X., Ali, S., Manzoor, M. A., Ur Rahman, F., Alam, P., & Qin, Y. (2026). Transcriptome profiling reveals γ-aminobutyric acid-mediated alleviation of chilling injury in pitaya via regulation of phenylpropanoid and phytohormone signaling pathways. *Plant Physiol Biochem*, *236*, 111439. https://doi.org/10.1016/j.plaphy.2026.111439

Shahzad, A., Sun, M., Pei, S., Liu, X., Zhang, Y., Xu, K., Gao, H., Zhou, Y., & Li, H. (2026). Decoding stress resilience in soybean: Regulatory networks and precision breeding under climate change. *J Integr Plant Biol*. https://doi.org/10.1111/jipb.70248

Shen, J., Xu, Y., Yuan, S., Jin, F., Huang, Y., Chen, H., Shan, Z., Yang, Z., Chen, S., Zhou, X., & Zhang, C. (2023). Genome-Wide Identification of GmSPS Gene Family in Soybean and Expression

Analysis in Response to Cold Stress. *Int J Mol Sci*, *24*(16). https://doi.org/10.3390/ijms241612878

Shi, Q., Mo, W., Zheng, X., Zhao, X., Chen, X., Zhang, L., Qin, J., Yang, Z., & Zuo, Z. (2025). Balancing act: progress and prospects in breeding soybean varieties with high oil and seed protein content. *Front Plant Sci*, *16*, 1560845. https://doi.org/10.3389/fpls.2025.1560845

Shomo, Z. D., Li, F., Smith, C. N., Edmonds, S. R., & Roston, R. L. (2024). From sensing to acclimation: The role of membrane lipid remodeling in plant responses to low temperatures. *Plant Physiol*, *196*(3), 1737-1757. https://doi.org/10.1093/plphys/kiae382

Su, L. T., Li, J. W., Liu, D. Q., Zhai, Y., Zhang, H. J., Li, X. W., Zhang, Q. L., Wang, Y., & Wang, Q. Y. (2014). A novel MYB transcription factor, GmMYBJ1, from soybean confers drought and cold tolerance in Arabidopsis thaliana. *Gene*, *538*(1), 46-55. https://doi.org/10.1016/j.gene.2014.01.024

Sun, L., Li, X., Wang, Z., Sun, Z., Zhu, X., Liu, S., Song, F., Liu, F., & Wang, Y. (2018). Cold Priming Induced Tolerance to Subsequent Low Temperature Stress is Enhanced by Melatonin Application during Recovery in Wheat. *Molecules*, *23*(5). https://doi.org/10.3390/molecules23051091

Tsegaw, M., Zegeye, W. A., Jiang, B., Sun, S., Yuan, S., Han, T., & Wu, T. (2023). Progress and Prospects of the Molecular Basis of Soybean Cold Tolerance. *Plants (Basel)*, *12*(3). https://doi.org/10.3390/plants12030459

Vianna, G. R., Cunha, N. B., & Rech, E. L. (2023). Soybean seed protein storage vacuoles for expression of recombinant molecules. *Curr Opin Plant Biol*, *71*, 102331. https://doi.org/10.1016/j.pbi.2022.102331

Wang, X., Yu, C., Liu, Y., Yang, L., Li, Y., Yao, W., Cai, Y., Yan, X., Li, S., Cai, Y., Li, S., & Peng, X. (2019). GmFAD3A, A ω-3 Fatty Acid Desaturase Gene, Enhances Cold Tolerance and Seed Germination Rate under Low Temperature in Rice. *Int J Mol Sci*, *20*(15). https://doi.org/10.3390/ijms20153796

Zhang, H., Dong, J., Zhao, X., Zhang, Y., Ren, J., Xing, L., Jiang, C., Wang, X., Wang, J., Zhao, S., & Yu, H. (2019). Research Progress in Membrane Lipid Metabolism and Molecular Mechanism in Peanut Cold Tolerance. *Front Plant Sci*, *10*, 838. https://doi.org/10.3389/fpls.2019.00838

Zhang, L., Wang, S., Bai, B., Chen, Y., Xiang, Z., Chen, C., Kuang, X., Yang, Y., Fu, J., Chen, L., & Mao, D. (2024). OsKASI-2 is required for the regulation of unsaturation levels of membrane lipids and chilling tolerance in rice. *Plant Biotechnol J*, *22*(8), 2157-2172. https://doi.org/10.1111/pbi.14336

Zhang, X., Feng, Y., Wang, Y., Xu, X., Wang, Y., Zhang, F., Zhang, L., & Liu, Q. (2025). Genetic Modulation of ROS Scavenging by DgNAC3 Improves Cold Stress Tolerance in Chrysanthemum morifolium. *Physiol Plant*, *177*(5), e70593. https://doi.org/10.1111/ppl.70593

Zhang, X. W., An, X. H., Xu, R. R., Tian, Y., Liu, B., Han, Y., & An, J. P. (2025). The MdGLK1-MdBZR1 Module Integrates Ethylene and Strigolactone Signals to Regulate Cold Tolerance via a CBF-Dependent Pathway in Apple. *Plant Biotechnol J*, *23*(12), 5550-5569. https://doi.org/10.1111/pbi.70325

Zhang, Y., Ming, R., Khan, M., Wang, Y., Dahro, B., Xiao, W., Li, C., & Liu, J. H. (2022). ERF9 of Poncirus trifoliata (L.) Raf. undergoes feedback regulation by ethylene and modulates cold tolerance via regulating a glutathione S-transferase U17 gene. *Plant Biotechnol J*, *20*(1), 183-200. https://doi.org/10.1111/pbi.13705

Zhong, S., Shi, H., Xue, C., Wei, N., Guo, H., & Deng, X. W. (2014). Ethylene-orchestrated circuitry coordinates a seedling's response to soil cover and etiolated growth. *Proc Natl Acad Sci U S A*, *111*(11), 3913-3920. https://doi.org/10.1073/pnas.1402491111

Zhou, L., Ullah, F., Zou, J., & Zeng, X. (2025). Molecular and Physiological Responses of Plants that Enhance Cold Tolerance. *Int J Mol Sci*, *26*(3). https://doi.org/10.3390/ijms26031157

Supplementary Files

This is a list of supplementary files associated with this preprint. Click to download.

- SupplementaryFile.docx